Thermal study of variable conductivity and variable viscosity considering magnetic dipole on nanofluid flow with heat sink/source

Munazza Saeed*,[1], Madiha Rashid[2], Muavia Mansoor[1] and Muhammad Irfan*,[3]

[1] Department of Mathematics, University of Wah, Wah Cantt, Pakistan

[2]Skyline University College, Sharjah, United Arab Emirates (UAE)

[3]Department of Mathematical Sciences Federal Urdu University of Arts, Sciences & Technology, Islamabad 44000, Pakistan

Corresponding Email: Munazza.saeed@uow.edu.pk (Munazza Saeed)

mirfan@math.qau.edu.pk (Muhammad Irfan)

Abstract: The goal of the current study is to examine how the magnetic dipole effects on nanofluid flow over an extended surface. Based on a constant, non-porous material with a velocity slip condition, this investigation has been reported. The effects of the variable viscosity and thermal conductivity are explored for two different types of nanofluids. The experiment's findings involved dispersing in water and ethylene glycol base solutions. For both types of nanofluids, the fundamental governing equations are converted into nonlinear ordinary differential equations using the suitable transformation and solved using the bvp4c technique. The viscosity and porosity parameters decay the velocity field. Furthermore, the transport of heat is decaying function of viscous dissipation factor, growing function of Prandtl factor.

Keywords: Magnetic dipole; Variable viscosity, Nanofluid, Porous medium, Newtonian heating; Heat sink/source

1. Introduction

Currently, nanofluids have concerned a boundless deal of consideration because of their prospective in increasing the heat transport. The nano-sized metallic elements, that is, gold, iron, copper, aluminum, or their oxides are utilized as colloidal representatives with greatest collective base liquids for instance, glycol, water, ethylene, or lubricant so that value-added thermo-physical

aspects of heat transport of base fluid. Choi and Eastman [1] established a brand-new type of fluid named nanofluid. Nanofluids have uses in a number of industries, comprising transportation, energy production, electrical structures like microprocessors, and biology. Numerous scholars have looked into the topic of nanofluids both mathematically and experimentally for heat transport characteristics. The studies related to nanofluid are explored in Refs. [2-11]. Furthermore, Manigandan and Narayana [12] examined variable properties of thermal conductivity on hybrid nanofluid with slip mechanisms. Irfan [13] elaborated Joule heating influence and activation energy in Maxwell nanofluid.

Furthermore, an innovative kind of nanofluid that has newly been used in research is a hybrid nanofluid. It is formed by dissolving two different kinds of nanoparticles throughout the base fluid. The rapid growth of theoretical studies has led to the proposal of many new mathematical models. Scientists and researchers formed hybrid ferrofluids, which have nanoparticles distributed throughout, in an effort to increase fluid efficiency. However, a study of the works reveals that only a small number of studies [14–17] have concentrated on the flow and heat transmission of hybrid ferrofluids. Research on MHD hybrid ferrofluid and the impact of erratic heat sources and sinks on the flow of radiative thin films was suggested by Kumar et al. [18]. Tlili et al. [19] studied MHD hybrid ferrofluid under the impact of asymmetrical heat (rise/fall) was then continued. Manhet al. [20] investigated the role of radiation in the heat transmission of an MHD hybrid ferrofluid submerged in porous media. In a mixed convection flow on a hybrid ferrofluid $(Fe_3O_4 - CoFe_2Fe_2)$, Zainodin et al. [21] examined exponentially deformable sheets at stagnation points with the effects of heat source/sink and velocity slip.

The study analysis of the works revealed that no study of hybrid nanoparticles that affect the thermal growth of heat in ferrofluid when it is exposed to a magnetic dipole. The mathematical model by Tiwari and Das [22] has been employed to address this issue. The current article explores the theory of nanofluid [23-25] in view of convective conditions on ferro-magnetic hybrid nanofluid [26-27] with variable viscosity [28-32], thermal conductivity in porous surface considering magnetic dipole. The bvp4c method utilized for solutions.

2. Description of the problem

Here the flow of ferromagnetic nanofluid $\left(\gamma Al_2O_3\ H_2O, \gamma Al_2O_3\ C_2H_6O_3\right)$ along stretched surface is taken into consideration. This flow is stable, two-dimensional, and incompressible.

2.1.Model assumptions and conditions

The following assumptions are taken into account when analyzing the mathematical model:

- Nanoparticles
- Variable thermal conductivity
- Magnetic dipole
- Varying viscosity
- Porous substance
- Heat sink/source

The sheet is stretched with velocity $U_\omega = cx$ denotes the velocity of the extended sheet. The temperature T of a fluid temperature of the surface and T_ω and T_c denote the initial and ambient temperatures, respectively, i.e., $T_\omega < T_\infty < T_c$. The magnetic dipole study are also considered shown in Fig.[1].

The governing equations are

$$\frac{\partial u}{\partial x} + \frac{\partial v}{\partial y} = 0 \qquad (1)$$

$$\rho_{nf}\left(u\frac{\partial u}{\partial x} + v\frac{\partial v}{\partial y}\right) = \frac{\partial}{\partial y}\left(\mu_{nf}\left(T\right)\frac{\partial u}{\partial y}\right) + \mu_0 M\frac{\partial H}{\partial x} - \frac{\varepsilon \nu_{nf}}{k}u \qquad (2)$$

$$\left(u\frac{\partial T}{\partial x} + v\frac{\partial T}{\partial y}\right) + \frac{\mu_0}{\left(\rho c_p\right)_{nf}}T\frac{\partial M}{\partial T}\left(u\frac{\partial H}{\partial x} + v\frac{\partial H}{\partial y}\right) = \frac{1}{\left(\rho c_p\right)_{nf}}\frac{\partial}{\partial y}\left(K_{nf}\left(T\right)\frac{\partial u}{\partial y}\right) + \frac{Q_0\left(T - T_c\right)}{\left(\rho c_p\right)_{nf}} \qquad (3)$$

Here μ_{nf}, $\rho_{nf}, \nu_{nf}, \varepsilon, K, \left(\rho c_p\right)_{nf}, K_{nf}$, M, H, c_p, Q_0 denotes the dynamic viscosity, density, kinematic viscosity, Porosity and permeability of porous medium, specific heat, thermal conductivity of the nanofluid, magnetization, magnetic field, specific heat and heat sink/source coefficient, respectively.

The boundary conditions are:

$$\left.u = U_\omega\left(x\right) = cx, v = 0, \frac{\partial T}{\partial y} = -h_s T\right\} at\ y = 0 \qquad (4)$$

$$u \to 0, v \to 0,\ T \to T_\infty = T_c \} \ when\ \ y \to \infty \qquad (5)$$

Here h_s the heat transfer coefficient.

The viscosity and thermal conductivity as an exponential function of temperature

$$\mu_f(T) = \mu_f\, exp\left[-a\left(T - T_c\right)\right] \qquad (6)$$

$$k(T) = k \exp\varepsilon\left(\frac{T_c - T}{T_c - T_\omega}\right) \qquad (7)$$

2.2.Thermo-physical properties of $\gamma Al_2O_3 - H_2O$ and $\gamma Al_2O_3 - C_2H_6O_3$:

A few features associated with nanofluids, their dynamic viscosity, effective density, specific heat capacity and thermal conductivity.

$$\mu_{nf}(T) = \frac{\mu_f \exp\left(-m_1\theta\right)}{\left(1-\varphi\right)^{2.5}},\ \rho_{nf} = \left(1-\varphi\right)\rho_f + \varphi\rho_s \qquad (8)$$

$$\left(\rho c_p\right)_{nf} = \left(1-\varphi\right)\left(\rho c_p\right)_f + \varphi\left(\rho c_p\right)_s \qquad (9)$$

$$k_{nf}(T) = \left(\frac{\left(k_s + 2k_f\right) - 2\varphi\left(k_f - k_s\right)}{\left(k_s + 2k_f\right) + \varphi\left(k_f - k_s\right)}\right) * k\left(\exp\varepsilon\left(\frac{T_c - T}{T_c - T_\omega}\right)\right) \qquad (10)$$

The relations determine the values of density, dynamic viscosity, specific heat and thermal conductivity of nanofluids. Base fluid and nanoparticles thermal conductivities are characterize as k_s *and* k_f, while φ denotes the volume of solid in the nanofluid , ρ_s *and* ρ_f represent the densities of the base fluid and nanoparticles, respectively.

2.3. Magnetic dipole

The magnetic field created by the magnetic dipole affects the flow of ferrofluid caused by stretching the sheet.

$\phi = \left(\frac{\gamma}{2\pi}\right)\left(\frac{x}{x^2 + \left(y+d\right)^2}\right)$ is the magnetic scalar potential of a ferrofluid. (11)

Here, γ denotes the strength of the magnetic field at the source, and d denotes the separation between the magnetic field's centre and the *x*-axis. H_x and H_y, which are defined as

$$H_x = -\frac{\partial \phi}{\partial x} = \left(\frac{\gamma}{2\pi}\right)\left(\frac{x^2 - (y+d)^2}{\left[x^2 + (y+d)^2\right]^2}\right) \tag{12}$$

$$H_y = -\frac{\partial \phi}{\partial y} = \left(\frac{\gamma}{2\pi}\right)\left(\frac{2x(y+d)}{\left[x^2 + (y+d)^2\right]^2}\right) \tag{13}$$

$$|H| = \left[\left(\frac{\partial \phi}{\partial x}\right)^2 + \left(\frac{\partial \phi}{\partial y}\right)^2\right]^{\frac{1}{2}} \tag{14}$$

$$\frac{\partial H}{\partial x} = -\left(\frac{\gamma}{2\pi}\right)\left(\frac{2x}{(y+d)^4}\right) \tag{15}$$

$$\frac{\partial H}{\partial y} = \left(\frac{\gamma}{2\pi}\right)\left(\frac{-2}{(y+d)^3} + \frac{2x^2}{(y+d)^5}\right) \tag{16}$$

Making use of the following similarity variables

$$\Psi(\zeta,\eta) = \left(\frac{\mu_f}{\rho_f}\right)\zeta f(\eta), \theta(\zeta,\eta) = \frac{T_c - T}{T_c - T_\omega} = \theta_1(\eta) + \zeta^2\theta_2(\eta), \eta = \left(\frac{\rho_f}{\mu_f}c\right)^{\frac{1}{2}} y\,, \tag{17}$$

$$\zeta = \left(\frac{\rho_f}{\mu_f}c\right)^{\frac{1}{2}} xu, = \frac{\partial \Psi}{\partial y} = cxf'(\eta)\,, v = -\frac{\partial \Psi}{\partial y} = -\sqrt{cv_f}\, f(\eta) \tag{18}$$

Equations [6-7] and [15-16] with [18-19] gives Eqs. [2 – 4]

$$\frac{(1-m_1\theta)\left[f''' - m_1\theta' f''\right]}{(1-\varphi)^{2.5}\left(1-\varphi+\varphi\frac{\rho_s}{\rho_f}\right)} - (f')^2 + ff'' = \frac{2\beta\theta_1}{\left(1-\varphi+\varphi\frac{\rho_s}{\rho_f}\right)(\eta+\alpha)^4} + \frac{\wedge_m f'}{\left(1-\varphi+\varphi\frac{\rho_s}{\rho_f}\right)} \tag{19}$$

$$\frac{\frac{k_{nf}}{k_f}(1+\theta_1)\theta_1''}{\left(1-\varphi+\varphi\frac{(\rho_s c_p)_s}{(\rho_f c_p)_f}\right)} + \frac{2\lambda\beta f}{(\eta+\alpha)^3}(\theta_1 -) + \Pr\left(f\theta_1' - 2f\theta_1'\right) - 4\lambda(f')^2 + \frac{Q_h}{\left(1-\varphi+\varphi\frac{(\rho c_p)_s}{(\rho c_p)_f}\right)}\theta_1 + PrQ_h\theta_1 = 0 \tag{20}$$

$$\frac{\frac{k_{nf}}{k_f}\left(1+\,_{\cdot}\theta_2\right)\theta_2''}{\left(1-\varphi+\varphi\frac{\left(\rho c_p\right)_s}{\left(\rho c_p\right)_f}\right)}+\frac{2\lambda\beta f}{\left(\eta+\alpha\right)^3}\theta_2-\lambda\beta\left(\theta_1-\,_{\cdot}\right)\left(\frac{2f'}{\left(\eta+\alpha\right)^4}+\frac{4f}{\left(\eta+\alpha\right)^5}\right)-\Pr\left(4f'\theta_2-f\theta_2'\right)-\lambda\left(f''\right)^2\frac{Q_h}{\left(1-\varphi+\varphi\frac{\left(\rho c_p\right)_s}{\left(\rho c_p\right)_f}\right)}\theta_2+PrQ_h\theta_2=0$$

(21)

subject to boundary conditions

$$f\left(\eta\right)=0\,,\,f'\left(\eta\right)=1,\theta_1'\left(\eta\right)=-\gamma_1\left(1+\theta_1\left(0\right)\right),\theta_2\left(\eta\right)=0\,at\,\eta=0, \tag{22}$$

$$f'\left(\eta\right)\to 0,\theta_1\left(\eta\right)\to 0,\theta_2\left(\eta\right)\to 0,\ when\,\eta\to\infty \tag{23}$$

Here (Prandtl number) Pr, (porosity parameter) $\wedge_m$, (Curie temperature ratio) $_{\cdot}$, (Newtonian heating parameter) γ_1, (Viscosity parameter) m, (Viscous dissipation) λ, (ferro hydrodynamic interaction parameter) β, (dimensionless distance) α and (heat sink/source) Q_h.

$$\begin{aligned}&Pr=\frac{k}{\alpha_f},\ \wedge_m=\frac{\varepsilon\nu_f}{kc}\,,\,_{\cdot}=\frac{T_\infty}{\left(T_c-T_\omega\right)},\gamma_1=h_s\sqrt{\frac{\nu_f}{c^2}}\ \ ,m=-a\left(T_c-T_\omega\right),\lambda=\frac{c\mu_f^2}{\rho K_1\left(T_c-T_\omega\right)}\\&\beta=\frac{\gamma\mu_0K_1\left(T_c-T_\omega\right)\rho_f}{2\pi\mu_f^2}\ ,\ \ \alpha=\sqrt{\frac{c\rho_fd^2}{\mu_f}},Q_h=\frac{Q_o}{c\left(\rho c_p\right)_{nf}}\end{aligned} \tag{24}$$

3. Physical interest

The Skin fraction and Local Nusselt mathematically as:

$$C_{fx}=\frac{-2\tau_\omega}{\rho_{nf}U_\omega^2}\,,\tau_\omega=\mu_{nf}\left(T\right)\frac{\partial u}{\partial y}|_{y=0} \tag{25}$$

$$Nu_x=\frac{xk_{nf}}{k_f\left(T_c-T_\omega\right)}\frac{\partial T}{\partial y}|_{y=0} \tag{26}$$

Dimensionless form

$$\frac{1}{2}\left(Re_x\right)^{\frac{1}{2}}C_{f_x}=\frac{\left(1-m_1\theta\left(0\right)\right)}{\left(1-\varphi\right)^{2.5}}\left(0\right),\left(Re_x\right)^{\frac{1}{2}}Nu_x=-\gamma_1\frac{k_{nf}}{k_f}\left(1+\frac{1}{\theta_1\left(0\right)+\zeta^2\theta_1\left(0\right)}\right) \tag{28}$$

where $Re_x=U_\omega\left(x\right)x/\nu_f$ is local Reynold number.

4. Discussion

Here numerical approach has been worked for solutions and present graphically and in tables form.

The values of fixed parameters taken are $\beta = 0.8$, $m_1 = Q_h = 0.1, \lambda = 0.01$, $\varphi = 0.15, \gamma_1 = 0.5$, $\wedge_m = 0.8$, $\gamma = 0.5$, $= 2, \Pr = 6.2$. Figures (2–5) elaborate on the implications $m_1, \beta, \wedge_m$ *and* γ_1 and on velocity profile. Figure 2 depicts the influence of viscosity change m_1 for the two nanofluids. This has dealt with a fall in Ferro-fluid velocity brought about by rise in exponential viscosity. The momentum boundary layer thickens as a result of the increase in viscous forces relative to inertial forces brought on by an upsurge in viscosity. Additionally, increasing the fluid's concentration through the inclusion of nanoparticles slows down the nanoliquid. The graph illustrates that, in the scenario of $\gamma Al_2O_3 - H_2O$ the fluid's velocity falls as the concentration of nanoparticles rises. The axial velocity of the nano fluid decreases when the density of the base fluid is increased with solid particles. The consequences of β are apparent in Figure 3. In the existence of $\gamma Al_2O_3 - H_2O$ and $\gamma Al_2O_3 - C_2H_6O_3$, as revealed in figure 3, the fluid viscosity increases and causes the axial velocity to decrease for increasing values of β. Figure 4 displays declining performance of $\wedge_m$ in flow of $\gamma Al_2O_3 - H_2O$ and $\gamma Al_2O_3 - C_2H_6O_3$ for the velocity distribution. Biological applications use porous media that contain pore structures filled with fluid. The γ_1 graph is explored in fig 5. The escalation in γ_1 alter the nanofluid axial velocity, which decreases velocity for γ_1. The impact of the viscosity parameter and the ferromagnetic parameter on the fluctuation in the temperature profile is explored by employing figures 6 and 7. The change in viscosity the resistive forces produced and results display the temperature rises. The temperature of the nanofluid is revealed to be elevated by deeper values of β as in Figure 7. This arises from the interaction of a magnetic field's action with nanoparticle motions, i.e., rise of temperature field caused decay in nanoparticle activities. Figures 8 and 9 illustrate a boost in Curie temperature relation, leading to an enhancement in the fluid's temperature profile. The influence of λ (viscous dissipation parameter) on the temperature contour is perceived in Figure 10. Regardless of the growing λ, it appears that the temperature contour improves. γ_1 impact on temperature profile reports in figure 11. Increase in γ_1 increase heat transport and intensifies temperature. Figure 12 illustrates a pattern towards cooling in the temperature profile. For higher quantities of $\Pr$, the temperature field drops. As thermal diffusivity falls, heat is isolated, missing from the heated sheet and enhancing the surface temperature gradient.

Thermo physical properties of nanomaterial are shown in **Table 1**. Numerical worth of skin friction

for two nanofluid for Pr , β , α parameter is provided in **Table 2**. The skin friction is increased by the higher levels of these limitations. Skin friction is exacerbated by a rise in resistance force attributed to an elevation in the volume fraction of nanoparticles and a greater range of magnetic restrictions. The consequence is comparatively prominent when $\gamma Al_2O_3 - H_2O$ nanofluid is employed. As shown in **Table 3**, larger values of Pr raise the cooling influence and, as a consequence, raise the Nusselt number, leading to greater skin friction and slow the heat transmission rate. Because of the $\gamma Al_2O_3 - C_2H_6O_3$ Nano fluid's strong thermo physical characteristics, cooling occurs quickly while Prandtl number is increased. The Nusselt number decreases as the hydrodynamic interaction constraint β and viscous dissipation term λ have rising values. The Nusselt number decreases as the amount of these parameters rises given that they physically enhance the Nano fluids' capacity to boost heat transfer. Also, **tables 2** and **3** characterize the comparison exploration in a limiting manner with the results of [33]. The discrepancy between numerical numbers and values from the literature demonstrates the applicability of the chosen technique whose step size has been set to h = 0.001 with an error tolerance of 10^{-6} and has been meticulously designed for convergence.

5. Conclusion

Here the magnetic dipole in ferromagnetic flow considering nanofluid has been examined numerically. The aluminum oxide nanoparticles utilizing water and ethylene glycol as the base fluid with variable viscosity and thermal conductivity have also studied. The key insight of the mentioned paper is

- The velocity profile was decreased by altering the viscosity parameter, while temperature profile enhanced.
- Temperature raised with higher values of the Curie temperature ratio, and temperature of the fluid decayed with increasing values of the Prandtl number.
- The temperature field enhanced for the rising value of ferromagnetic interaction factor.
- Up surging values of Curie temperature parameter raised the temperature field.
- The increasing λ and λ_1 caused the temperature field to become stronger, and that the nanofluid $\gamma Al_2O_3 - H_2O$ has a relatively better influence on this consequence.

References

1. Choi, S.U., and Eastman, J.A., ‘’Enhancing thermal conductivity of fluids with nanoparticles’’, *ASME J. Heat Transf.,* 66, 99-105 (1995).
2. Buongiorno, J., ‘’Convective transport in nanofluids’’, *J. Heat. Tranf.,* 128, 240-250 (2006) https://doi.org/10.1115/1.2150834.
3. Khan, W.A., and Pop, I., ‘’Boundary-layer flow of a nanofluid past a stretching sheet’’, *Int. J. Heat Mass Transf.,* 53, 2477-2483 (2010) https://doi.org/10.1016/j.ijheatmasstransfer.2010.01.032.
4. Kuznetsov, A., and Nield, D., ‘’The Cheng-Minkowycz problem for natural convective boundary layer flow in a porous medium saturated by a nanofluid: a revised model’’, *Int. J. Heat Mass Transf.,* 65, 682-685 (2013) https://doi.org/10.1016/j.ijheatmasstransfer.2013.06.054.
5. Hamid, A., Hashim and Khan, M., Impacts of binary chemical reaction with activation energy on unsteady flow of magneto-Williamson nanofluid, *J. Mol. Liq.,* 262, 435-442 (2018) https://doi.org/10.1016/j.molliq.2018.04.095.
6. Khan, M., Hamid, A., and Hashim, ‘’Effects of thermal radiation and slip mechanism on mixed convection flow of Williamson nanofluid over an inclined stretching cylinder’’, *Commun. Theor. Phys.,* 71, 1405 (2019) https://doi.org/10.1088/0253-6102/71/12/1405.
7. Ferdows, M., Zaimi, K., Rashad, A.M., and Nabwey, H.A., ‘’MHD bioconvection flow and heat transfer of nanofluid through an exponentially stretchable sheet’’, *Symmetry,* (2020) https://doi.org/10.3390/sym12050692.
8. Song, Y.Q., Hamid, A., Sun, T.C., et al., ‘’Unsteady mixed convection flow of magneto-Williamson nanofluid due to stretched cylinder with significant non-uniform heat source/sink features’’, *Alexandria Eng. J.,* 61, 195–206 (2022) https://doi.org/10.1016/j.aej.2021.04.089.
9. Ali, U., Irfan, M., Akbar, N.S., et al., ‘’Dynamics of soret–dufour effects and thermal aspects of Joule heating in multiple slips Casson–Williamson nanofluid’’, *Int. J. Modern Physics B,* (2023) https://doi.org/10.1142/S0217979224502060.
10. Anwar, M.S., Muhammad, T., Khan, M., et al., ‘’MHD nanofluid flow through darcy medium with thermal radiation and heat source’’, *Int. J. Modern Phy. B,* (2023) https://doi.org/10.1142/S0217979224503867.

11. Irfan, M., Anwar, M.S., Kebail, I., and Khan, W.A., ‘’Thermal study on the performance of Joule heating and Sour-Dufour influence on nonlinear mixed convection radiative flow of Carreau nanofluid’’, *Tribology Int.,* 188, 108789 (2023) https://doi.org/10.1016/j.triboint.2023.108789.
12. Manigandan, A., and Narayana, P.V.S., ‘’Influence of variable thermal conductivity and mixed convection on hybrid nanofluid (SWCNT + MWCNT/H2O) flow over an exponentially elongated sheet with slip conditions’’, *Indian J. Phy.,* (2023) https://doi.org/10.1007/s12648-023-02912-8.
13. Irfan, M,. ‘’Energy transport phenomenon via Joule heating and aspects of arrhenius activation energy in maxwell nanofluid’’, *Waves Random Complex Media,* (2023) https://doi.org/10.1080/17455030.2023.2196348.
14. Shah, F., Khan, S.A., K. Al-Khaled, Khan, M.I., et al., ‘’Impact of entropy optimized darcy-forchheimer flow in MnZnFe2O4 and NiZnFe2O4 hybrid nanofluid towards a curved surface’’, Zeitschrift für Angewandte Mathematik und Mechanik, 102, (2021) https://doi.org/10.1002/zamm.202100194.
15. Ahmad, H., Al-Khaled, K., Sowayan, A.S., et al., ‘’Experimental investigation for automotive radiator heat transfer performance with ZnO-Al2O3/water based hybird nanoparticles: An improved thermal model’’, *Int. J. Modern Physics B,* 37, 2350050 (2023) https://doi.org/10.1142/S0217979223500509.
16. Shamshuddin, M.D., Saeed, A., Mishra, S.R., et al., ‘’Homotopic simulation of MHD bioconvective flow of water-based hybrid nanofluid over a thermal convective exponential stretching surface’’, *Int. J. Numer. Methods for Heat Fluid Flow,* (2023) https://doi.org/10.1108/HFF-03-2023-0128.
17. Rehman, M.S.U., Chen, H., et al., ‘’Thermal analysis of radiative and electromagnetic flowing of hybridity nanofluid via darcy–forchheimer porous material with slippage constraints’’, *Energy Envoirment,* (2023) https://doi.org/10.1177/0958305X231196298.
18. Kumar, K.A., Sandeep, N., Sugunamma, V., and Animasaun, I.L., ‘’Effect of irregular heat source/sink on the radiative thin film flow of MHD hybrid ferrofluid’’, *J. Therm. Anal. Calorim.,* 139, 2145-2153 (2020) https://doi.org/10.1007/s10973-019-08628-4.

19. Tlili, I., Mustafa, M.T., Kumar, K.A., and Sandeep, N., ‘’Effect of asymmetrical heat rise/fall on the film flow of magnetohydrodynamic hybrid ferrofluid’’, *Sci. Rep.*, 10, 1-12 (2020) https://doi.org/10.1038/s41598-020-63708-y.
20. Manh, T.D., Khan, A.R., Shafee, A., et al., ‘’Hybrid nanoparticles migration due to MHD free convection considering radiation effect’’, *Physica A*, 551 (2020) https://doi.org/10.1016/j.physa.2019.124042.
21. Zainodin, S., Jamaludin, A., Nazar, R., et al., ‘’MHD mixed convection of hybrid ferrofluid flow over an exponentially stretching/shrinking surface with heat source/sink and velocity slip’’, *Mathematics*, 10, 4400 (2022) https://doi.org/10.3390/math10234400.
22. Tiwari, R.K., Das, M.K., ‘’Heat transfer augmentation in a two-sided lid-driven differentially heated square cavity utilizing nanofluids’’, *Int. J. Heat Mass Transf.*, 50, 2002-2018 (2007) https://doi.org/10.1016/j.ijheatmasstransfer.2006.09.034.
23. Yang, H., Majeed, A., A.K., Kamel, Saeed, M., ‘’Significance of melting heat transfer and brownian motion on flow of powell-eyring fluid conveying nano-sized particles with improved energy systems’’, *Lubricants*, 11, (2023) https://doi: 10.3390/lubricants11010032.
24. Rehman, M.I., Chen, H., Hamid, A., et al., ‘’Thermal and solutal slip impacts of tribological coatings on the flow and heat transfer of reiner-philippoff nanofluid lubrication toward a stretching surface: The applications of Darcy-Forchheimer theory’’, *Tribology Int.*, 190, 109038 (2023) https://doi.org/10.1016/j.triboint.2023.109038.
25. Rehman, M.I., Chen, H., Hamid, A., et al., ‘’Numerical analysis of unsteady non-linear mixed convection flow of reiner-philippoff nanofluid along falkner-skan wedge with new mass flux condition’’, *Chemical Phy. Letters*, 830, 140799 (2023) https://doi.org/10.1016/j.cplett.2023.140799.
26. Irfan, M., Khan, W.A., et al., ‘’Significance of non-fourier neat flux on ferromagnetic powell-eyring fluid subject to cubic autocatalysis kind of chemical reaction’’, *Int. Comm. Heat Mass Transfer*, 138, 106374 (2022) https://doi.org/10.1016/j.icheatmasstransfer.2022.106374.
27. Hussain, I., Khan, W.A., Tabrez, M., et al., ‘’Dynamics of stratifications and magnetic dipole for radiative flow of ferromagnetic Sutterby fluid’’, *(ZAMM) J. Appl. Mathematics Mechanics*, 103, e202200226 (2023) https://doi.org/10.1002/zamm.202200226.

28. Saeed, M., Ahmad, B., Hassan, Q.M.U., ‘’Variable thermal effects of viscosity and radiation of ferrofluid submerged in porous medium’’, *Ain Shams Eng. J.*, 2021, 101653 (2021) https://doi.org/10.1016/j.asej.2021.101653.
29. Kumar, S.B., Shankar, B.M., Latha, N., et al. ‘’Instability thresholds for penetrative porous convection with variable viscosity fluids’’, *Int. Commun. Heat Mass Transf.*, 149, 107056 (2023) https://doi.org/10.1016/j.icheatmasstransfer.2023.107056.
30. Shankar, B.M., Nagamani, K.V., and Shivakumara, I.S., ‘’Further thoughts on buoyancy-induced instability of a variable viscosity fluid saturating a porous slab’’, *Physics of Fluids,* 35 (2023) https://doi.org/10.1063/5.0158115.
31. Shankar, B.M., Nagamani, K.V., and Shivakumara, I.S., ‘’Stability of flow of a variable-viscosity fluid saturating a differentially heated vertical porous layer’’, *Transport in Porous media,* 150, 1-14 (2023) https://doi.org/10.1007/s11242-023-01975-9.
32. Tripathi, V.K., Shankar, B.M., Mahajan, A., et al., ‘’Global nonlinear stability of bidispersive porous convection with throughflow and depth-dependent viscosity’’, *Phy. Fluids,* 36, 014110 (2024) https://doi.org/10.1063/5.0174734.
33. Abbas, K., Taza, G., Taza , et al., ‘’The flow of ferromagnetic nanofluid over an extending surface under the effect of operative Prandtl model’’, *Advances Mech. Eng.*, 2019, https://doi.org/10.1177/1687814019896128.

Biographies

Munazza Saeed is a lecturer at the University of Wah, Pakistan. She received PhD degree in mathematics in the field of fluid mechanics University of Wah, Pakistan. Her research interests included is fluid mechanics and published 19 research articles appear in reputed international journals.

Madiha Rashid is an instructor at Skyline University College, Sharjah, United Arab Emirates. He received PhD degree in Mathematics in the field of Fluid Mechanics, Quaid-i-Azam University Islamabad, Pakistan. His research interests included is Fluid Mechanics and published 15 research articles appear in reputable international journals.

Muavia Mansoor is a lecturer at the University of Wah, Pakistan. He received PhD degree in mathematics in the field of fluid mechanics, University of Wah, Pakistan. His research interests included is fluid mechanics and published 14 research articles appear in reputed international journals.

Muhammad Irfan is an Assistant professor at Federal Urdu University of Arts Sciences and Technology, Islamabad, Pakistan. He received PhD degree in Mathematics in the field of Fluid Mechanics, Quaid-i-Azam University Islamabad, Pakistan. His research interests included is Fluid Mechanics and published 119 research articles appear in reputable international journals.

List of Figures

Fig. 7 Graph of β verses $\theta_1(\eta)$

Fig. 8 Graph of φ verses $\theta_1(\eta)$

Fig. 9 Graph of φ verses $\theta_2(\eta)$

Fig. 10 Graph of λ verses $\theta_1(\eta)$

Fig. 11 Graph of γ_1 verses $\theta_2(\eta)$

Fig. 12 Graph of Pr verses $\theta_1(\eta)$

List of Tables:

Table 1: List of the current study's (thermo-physical characteristics).

Contents	*Density*	*Specific heat*	*Thermal conductivity*
Water (H_2O)	*998.3*	*4182*	*0.6*
Ethylene glycol $(C_2H_6O_3)$	*1116.6*	*2382*	*0.249*
Gamma-alumina (γAl_2O_3)	*3970*	*765*	*40*

Table 2: shows numerical quantities of skin friction coefficient $\frac{1}{2}(Re_x)^{\frac{1}{2}} C_{f_x}$ for two nanofluids when $m_1 = 1, \lambda = 0.1, \varphi = 0.5$. Obtained results are compared with the results of Abbas Khan [33].

Khan et al. [33]					***Present***	
φ	β	α	$\gamma Al_2O_3 - H_2O$	$\gamma Al_2O_3 - C_2H_6O_3$	$\gamma Al_2O_3 - H_2O$	$\gamma Al_2O_3 - C_2H_6O_3$
0.01	*1*	*0.2*	*0.529705*	*0.52471*	*0.529700*	*0.52461*
0.03			*0.897501*	*0.879547*	*0.897491*	*0.879536*
0.05			*0.54147*	*0.50264*	*0.54137*	*0.50252*

	2		2.00877	1.96994	2.00863	1.96982
	3		2.47608	2.43724	2.47600	2.43711
		0.3	3.68432	3.1646	3.68421	3.1632
		0.4	4.68448	4.14641	4.68436	4.14653

Table 3: *Comparison of numerical results reported by of local Nusselt number for two nanofluids when* $\varphi = 0.1$, $\alpha = 0.2$, $= 0.5$.

Khan et al. [33]					**Present**	
Pr	β	λ	$\gamma Al_2O_3 - H_2O$	$\gamma Al_2O_3 - C_2H_6O_3$	$\gamma Al_2O_3 - H_2O$	$\gamma Al_2O_3 - C_2H_6O_3$
5.6	1	0.3	1.8123	1.89077	1.8112	1.89068
6.6			2.29341	2.39237	2.29331	2.39227
7.6			2.77451	2.89397	2.77462	2.89297
	2		1.85614	1.93647	1.85602	1.93637
	3		0.937765	0.978975	0.937763	0.978964
		0.35	0.47953	0.501218	0.479532	0.501207
		0.4	0.0212945	0.0234611	0.0212941	0.0234601

List of Figures

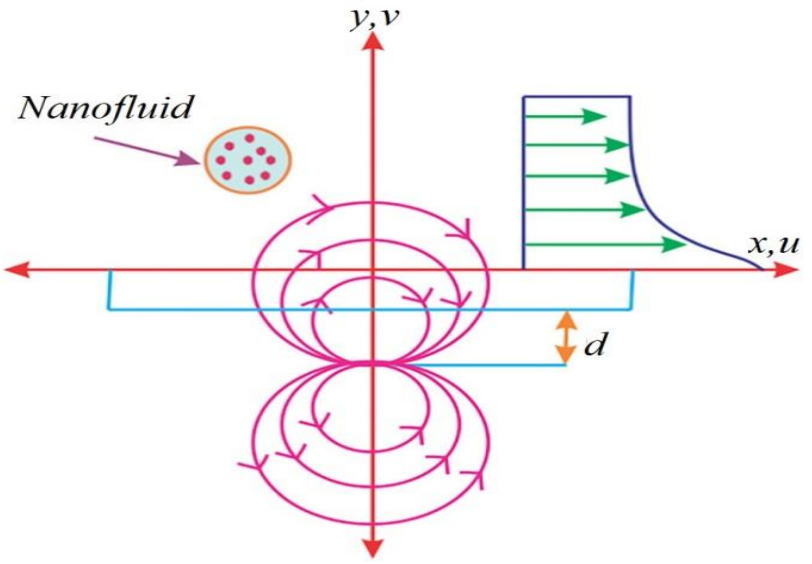
y, v
Nanofluid
x, u
d

Fig 1:

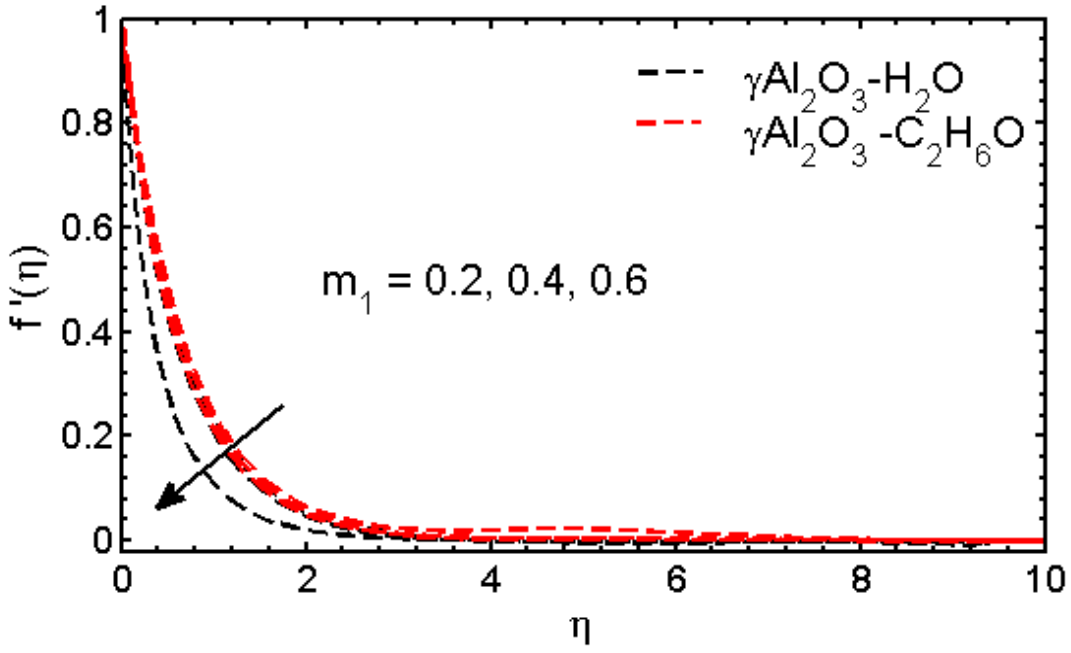
γAl2O3-H2O
γAl2O3 -C2H6O
m1 = 0.2, 0.4, 0.6
f '(η)
η
0
0.2
0.4
0.6
0.8
1
0
2
4
6
8
10

Fig 2:

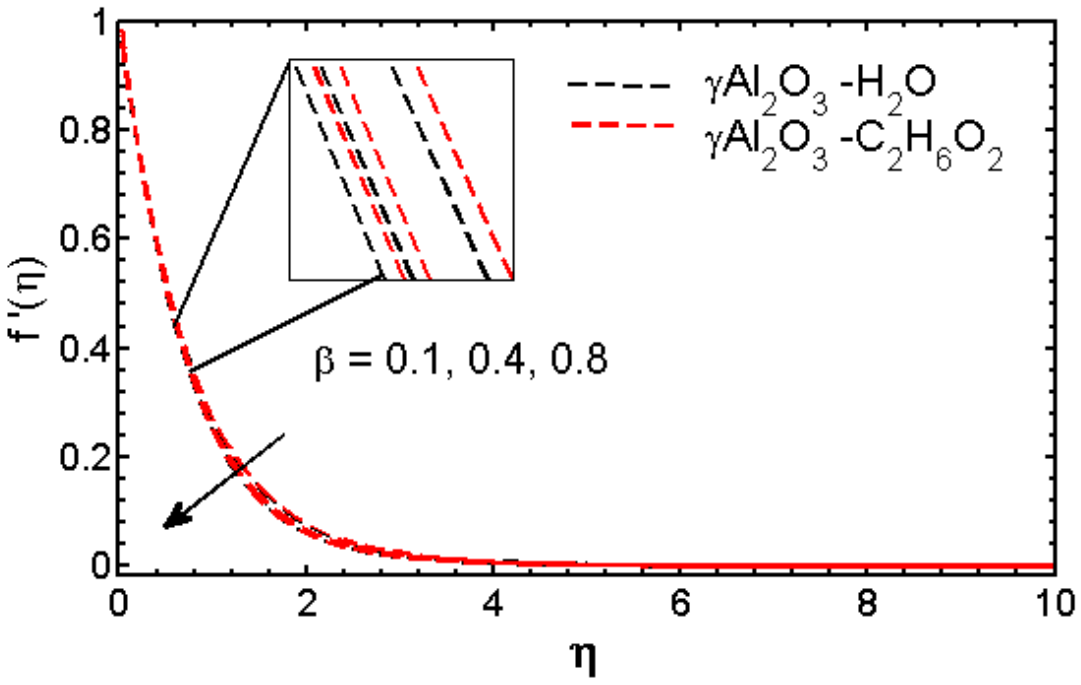
γAl2O3 -H2O
γAl2O3 -C2H6O2
β = 0.1, 0.4, 0.8
f '(η)
η
0
0.2
0.4
0.6
0.8
1
0
2
4
6
8
10

Fig 3:

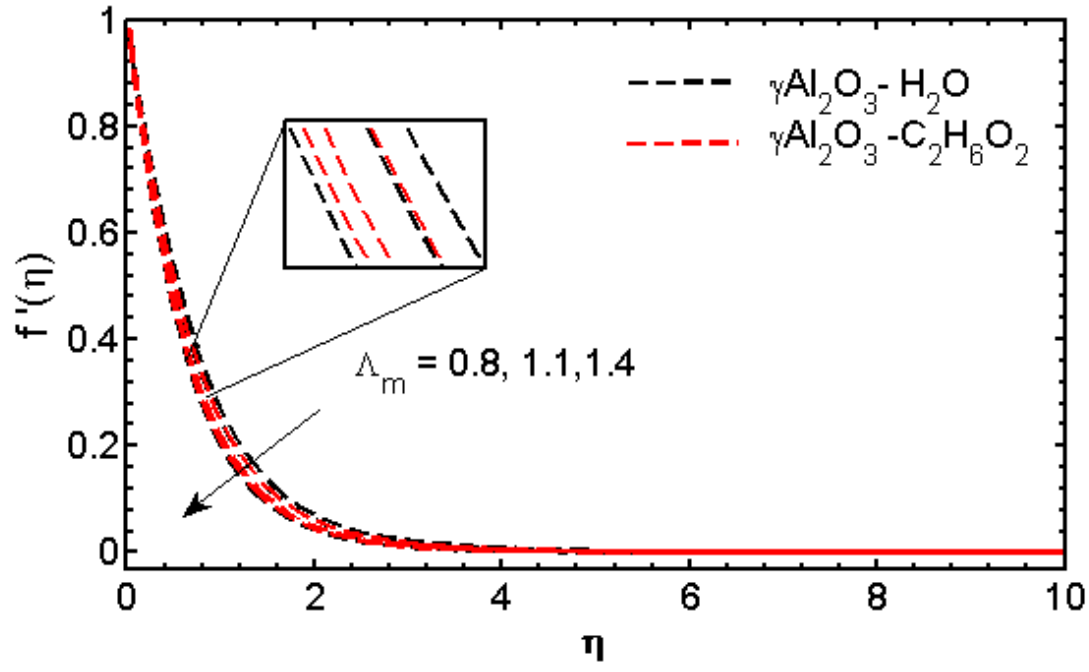
γAl2O3- H2O
γAl2O3 -C2H6O2
Λm = 0.8, 1.1,1.4
f '(η)
η
0
0.2
0.4
0.6
0.8
1
0
2
4
6
8
10

Fig 4:

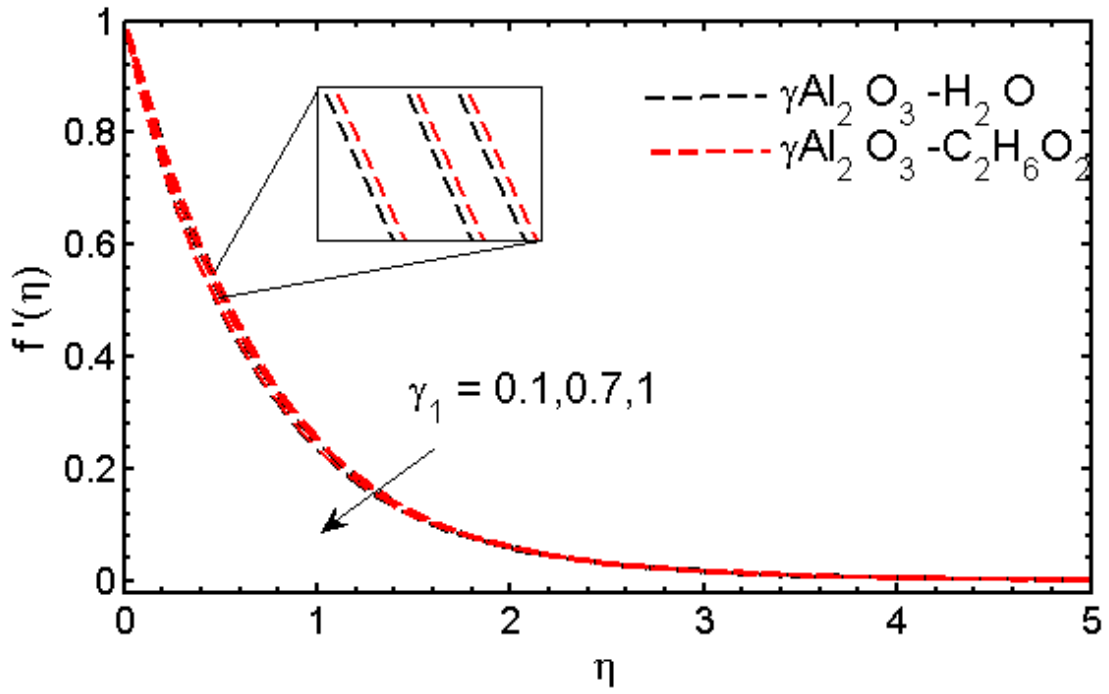
γAl2 O3 -H2 O
γAl2 O3 -C2H6O2
γ1 = 0.1,0.7,1
f '(η)
η

Fig 5

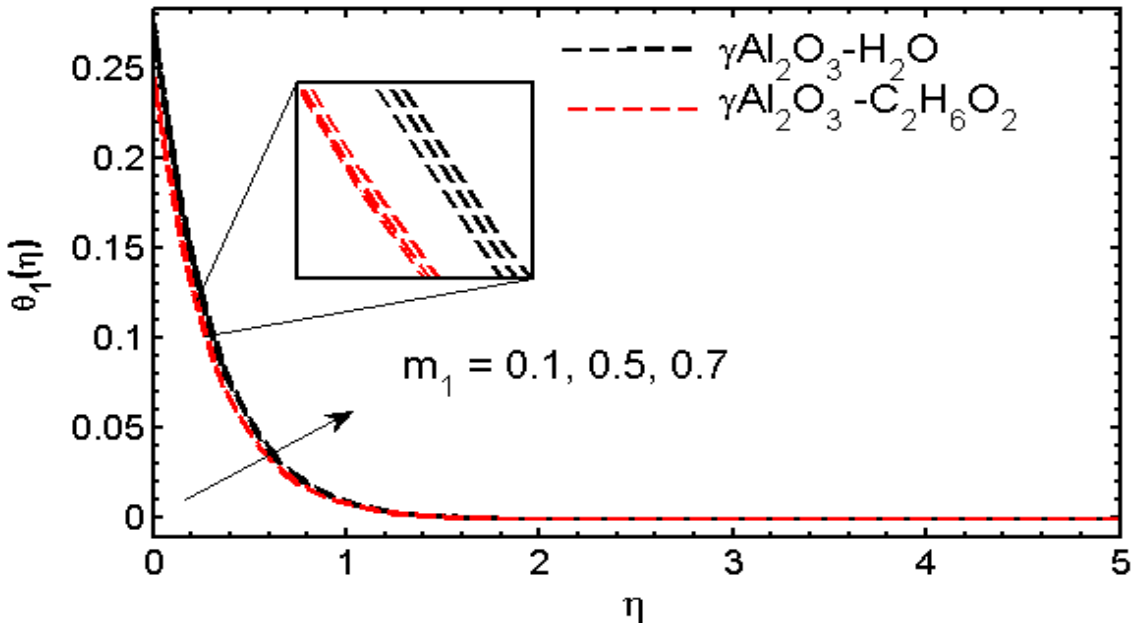
γAl2O3-H2O
γAl2O3 -C2H6O2
m1 = 0.1, 0.5, 0.7
θ1(η)
η

Fig 6:

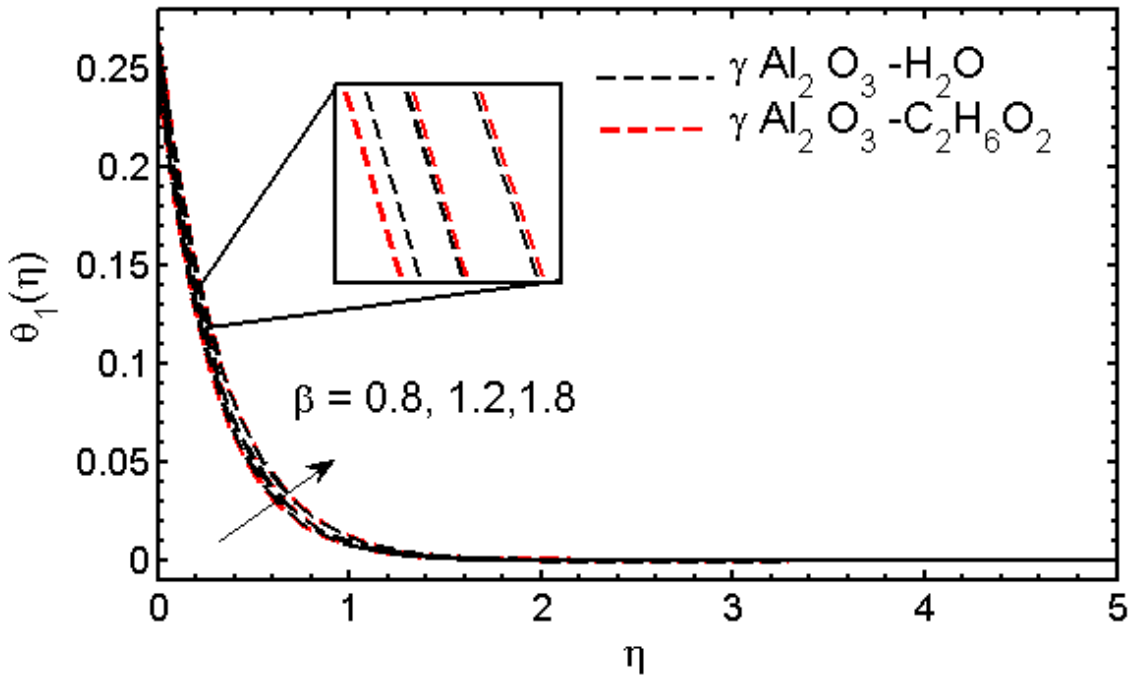

Fig 7:

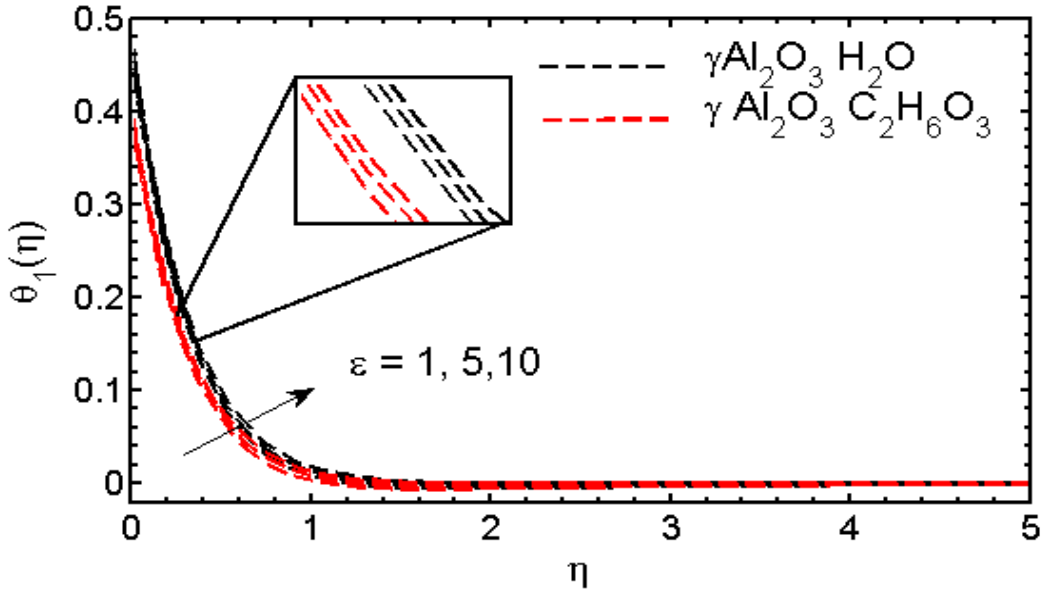

Fig 8:

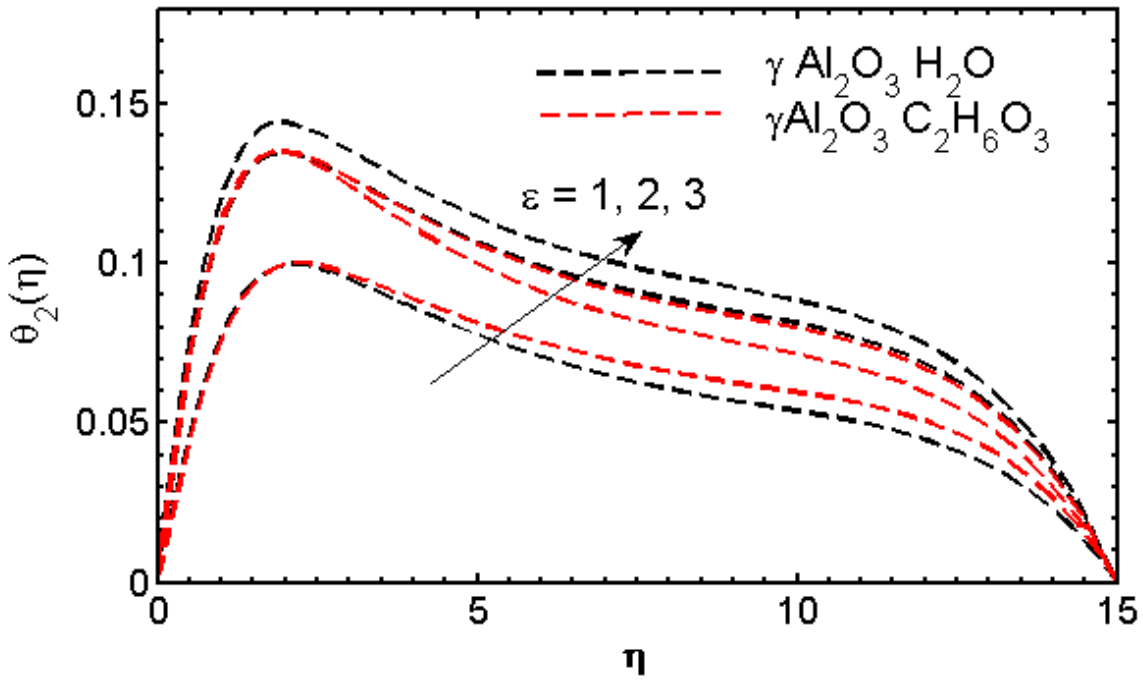
γ Al2O3 H2O
γAl2O3 C2H6O3
ε = 1, 2, 3
θ2(η)
η
0
0.05
0.1
0.15
0
5
10
15

Fig 9:

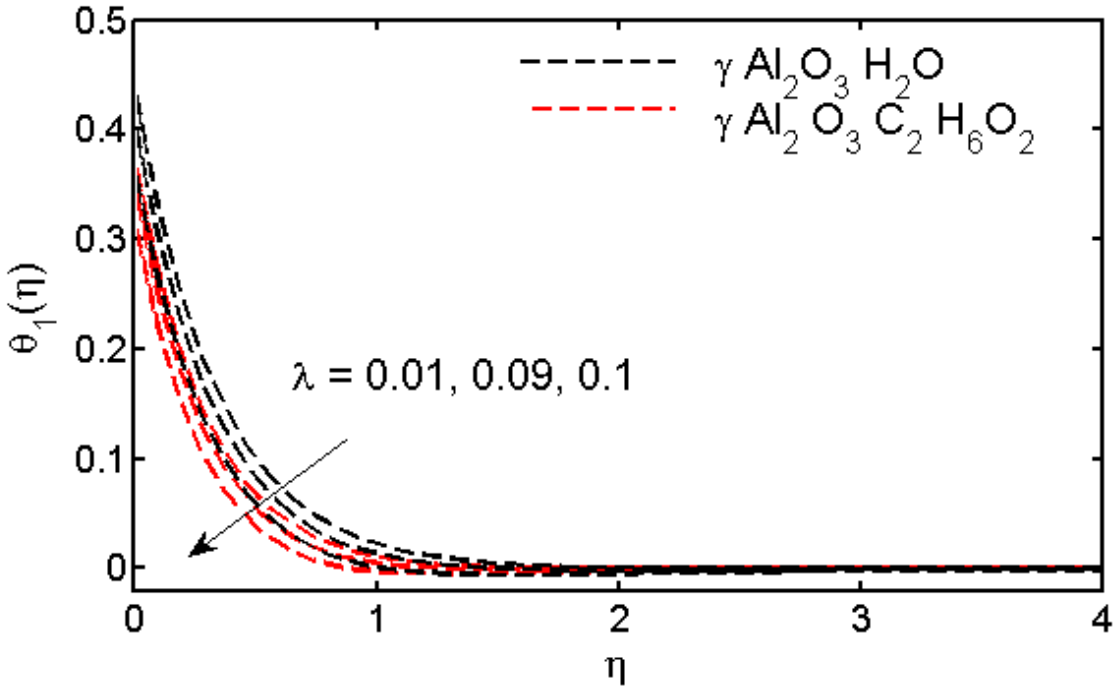
γ Al2O3 H2O
γ Al2 O3 C2 H6O2
λ = 0.01, 0.09, 0.1
θ1(η)
η
0
0.1
0.2
0.3
0.4
0.5
0
1
2
3
4

Fig 10:

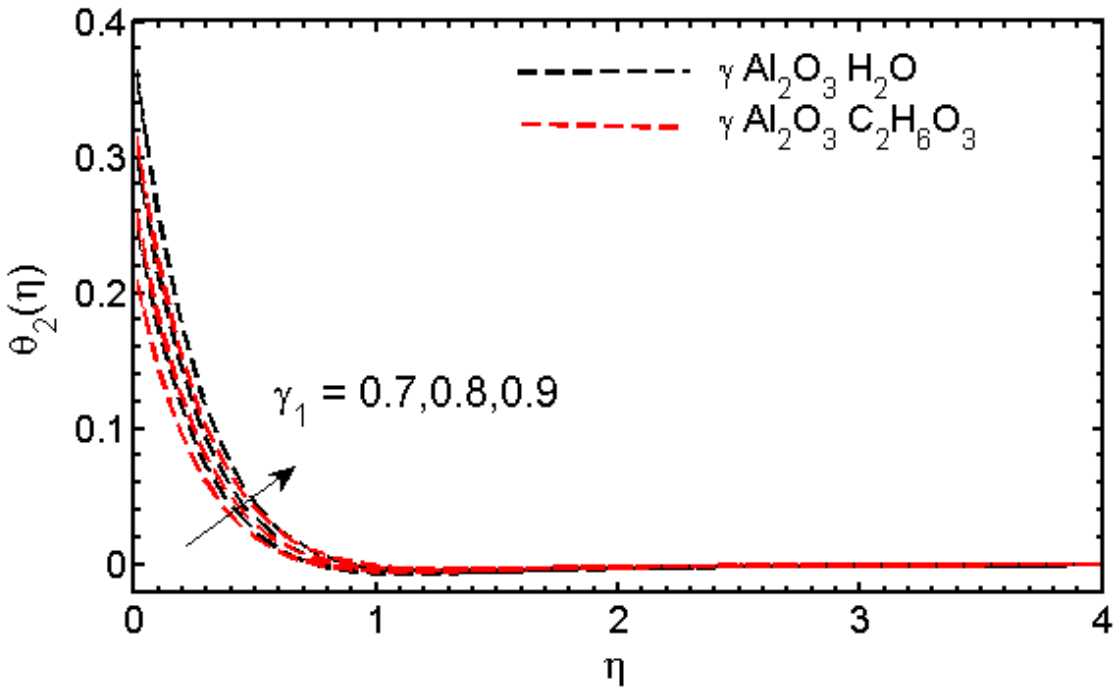
γ Al2O3 H2O
γ Al2O3 C2H6O3
γ1 = 0.7,0.8,0.9
θ2(η)
η
0.4
0.3
0.2
0.1
0
0
1
2
3
4

Fig 11:

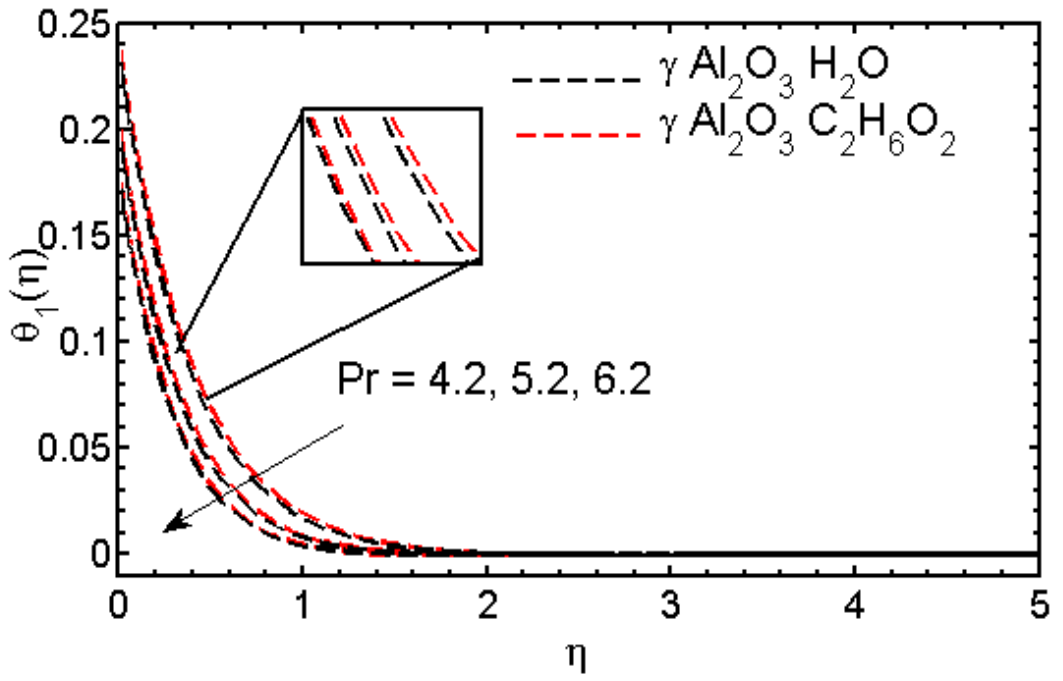
γ Al2O3 H2O
γ Al2O3 C2H6O2
Pr = 4.2, 5.2, 6.2
θ1(η)
η
0.25
0.2
0.15
0.1
0.05
0
0
1
2
3
4
5

Fig 12